Chemical Engineering Journal 437 (2022) 135274

Contents lists available at ScienceDirect

Chemical Engineering Journal

journal homepage: www.elsevier.com/locate/cej

Onion inspired hydrate-phobic surfaces

Feng Wang [a], Senbo Xiao [a], Jing He [b], Fulong Ning [c], Rui Ma [a], Jianying He [a,*], Zhiliang Zhang [a,*]

[a] NTNU Nanomechanical Lab, Department of Structural Engineering, Norwegian University of Science and Technology (NTNU), Trondheim 7491, Norway
[b] Key Lab of Photovoltaic and Energy Conservation Materials, Institute of Solid State Physics, HFIPS, Chinese Academy of Sciences, Hefei 230031, China
[c] Faculty of Engineering, China University of Geosciences, Wuhan, Hubei 430074, China

ARTICLE INFO

Keywords:
Onion film
Sub-surface pores
Gas hydrate
Hydrate-phobic surface
Adhesion strength

ABSTRACT

Hydrate plugging in gas- and oil-production and transport systems has long been a critical challenge. Traditional hydrate mitigation strategies through applying chemicals and thermal destabilization are costly and eco-unfriendly. Passive anti-hydrate surfaces with potential to enable self-removal of hydrates are desired. Surprisingly, thin onion film peeled off from an onion bulb scale is found to have low hydrate adhesion, thanks to the porous structures and the surface cuticle layer. Subsequently, through mimicking the bio-properties of an actual onion film, a hydrate-phobic onion inspired surface with super low hydrate adhesion strength is fabricated. By engineering abundant pores below smooth surface, the onion inspired surface dramatically decreases the cyclopentane (CyC5) hydrate adhesion strength from 95 kPa to 4.7 kPa. The onion inspired surface also maintains super low hydrate adhesion (8.7 kPa) after 20 hydrating/de-hydrating cycles. Furthermore, the performance of this new hydrate-phobic surface is enhanced by integrating a regenerable artificial cuticle layer, which enables even lower hydrate adhesion (2.9 kPa). Therefore, the onion inspired surface can provide alternative solutions for future hydrate mitigation.

1. Introduction

Natural gas hydrate is a promising future energy resource that consists of cage-like water skeleton with entrapped methane molecules [1,2]. Despite the great potentials of gas hydrates in numerous applications including gas storage [3], gas separation [4], desalination [5] and others, unwanted gas hydrate accumulation remains a challenge to gas- and oil-production and transport systems [6,7]. In the gas/oil pipeline systems, the hydrate plugs initiated by hydrate formation and deposition restrict the gas/oil flow, resulting in over-pressurization and other catastrophic consequences [8,9]. Avoiding hydrate plugging and further removing plugged hydrates safely have consumed a great amount of deep-water flow-assurance resources. State-of-the-art hydrate-plugging mitigation in the industry mainly relies on active methods by supplying thermal energy for hydrate melting or applying chemicals to inhibit hydrate formation [10–13]. However, these methods are energy-intensive, costly, and might also lead to environment problems [8,14,15]. In the last decade, increasing interests have been focused on passive anti-hydrate surfaces that can inhibit hydrate formation directly on pipe walls or lower hydrate adhesion for removal without external force or energy inputs [14,16–20].

Two major types of passive anti-hydrate coatings, namely polymeric and superhydrophobic coatings, are commonly investigated in the anti-hydrate communities. Firstly, the polymeric coatings are used to lower the hydrate adhesion strength [17,21,22]. Recently reported bilayer polymeric coatings developed through initiated chemical vapor deposition can decrease the adhesion strength of cyclopentane (CyC5) hydrate form ~220 kPa on rough steel to ~20 kPa [22]. Despite these pioneer polymeric coatings show promising hydrate-phobicity, surfaces with even lower hydrate adhesion strength (<10 kPa) are required for possible self-removal of hydrates [23,24]. Secondly, superhydrophobic coatings are employed for both inhibiting hydrate formation and reducing hydrate adhesion on surfaces [16,18,25–28]. Ideally, the superhydrophobic surfaces can enable Cassie-Baxter contact with hydrate precursor droplets atop and lead to the removal of hydrate particles with nondetectable force [25]. However, the application of superhydrophobic surfaces for hydrate mitigation is restricted owing to the known drawbacks of superhydrophobic surfaces for anti-icing [29–31]. On the one hand, the superhydrophobic surfaces gradually lose their functions in cyclic applications because of the degradation of surface micro-/nano- structures [29,30]. On the other hand, once the ice/hydrate form inside the textures of superhydrophobic surfaces, the

* Corresponding authors.
E-mail addresses: jianying.he@ntnu.no (J. He), zhiliang.zhang@ntnu.no (Z. Zhang).

https://doi.org/10.1016/j.cej.2022.135274
Received 16 November 2021; Received in revised form 5 February 2022; Accepted 12 February 2022
Available online 16 February 2022

mechanical inter-locking between ice/hydrates and substrates generates strong adhesion [31]. Therefore, novel anti-hydrate surfaces that can maintain durable low hydrate adhesion strength (<10 kPa) are desired.

Recently, it is suggested that anti-gas hydrate surfaces can be designed by learning from anti-icing surfaces [32]. Among the widely reported anti-icing surfaces, bio-inspired icephobic surfaces are among the most attractive strategies [33,34]. Despite that various surfaces from lotus-leaf inspired superhydrophobic surfaces (SHS) to pitcher-plants-inspired slippery liquid-infused porous surfaces (SLIPS) have been developed for multiple anti-icing applications [35,36], bio-inspired anti-hydrate surfaces is still in its infancy. The onion films that consist of monolayer epidermis cells can bend, contract and elongate and have shown potentials in artificial muscles [37]. However, the special adhesion behaviors of onion film have rarely been received attention. The onion film with microscale thickness (20–30 μm) [38] that maintains flexibility below 0 ℃ makes it a promising surface coating for anti-icing/anti-hydrate. In this work, for the first time, inspired by the onion, a novel anti-hydrate surface is designed. The essential mechanisms of onion films in lowering the adhesion between onion bulb scales is implanted in the as-prepared surface for practically low hydrate adhesion. The details of surface fabrication strategy for incubating low hydrate adhesion via sub-surface structures and surface lubrication are presented. The mitigated hydrate adhesion on the onion-inspired surface is discussed.

2. Results and discussions

2.1. Low hydrate adhesion on onion film

The unique adhesion behavior of onion bulb scales can be observed when an onion is put into freezing environment. As shown in the supplementary Fig. S1, a fresh onion contains plenty of water in its body and forms a compact block in a freezer. Surprisingly, even being fully frozen, onion bulb scales can be separated easily from each other. A more detailed investigation into the properties of the onion is then carried out to reveal the mechanism underlying the low adhesion between onion bulb scales. By focusing on an actual onion, we firstly take a look at the detail constitutes of the bulb scales. Interestingly, there is a special membrane, termed onion film in the following text, consists of monolayer epidermal cells between two onion bulb scales (supplementary Fig. S2) [39,40]. Since the onion film is the only tissue between two bulb scales, it is essential to firstly understand the adhesion behaviors of an onion film. As shown in Fig. 1a, the onion film can be peeled off easily from the bulb scales. Surprisingly, the onion film is hydrophobic thanks to a top cuticle layer of waxy polymer [41], with a water contact angle of ~103° (detailed information about contact angle characterization is given in supplementary Fig. S2). The onion film is comprised of special sub-surface structure and shapes of epidermal cells and pores, as resolved by scanning electron microscope (SEM) shown in Fig. 1b and c. The onion film is subjected to adhesion strength test for understanding of the essential mechanisms in the unique adhesion between bulb scales, as measurements shown in Fig. 1d. Specifically, onion bulb scales are firstly cut into cubes with a dimension of 10 mm * 10 mm * 2 mm. Onion cubes with and without an onion film are then placed onto glass substrates and are pressed with a weight atop. The systems are held in a freezer with internal temperature of −18 ℃ for 3 h before adhesion test. To measure the adhesion strength of onion bulb scales on substrates, shearing forces are applied on the frozen scales (inset, Fig. 1d). The adhesion strength is calculated using the monitored maximum shearing force normalized by the contact area (the same criteria is used for hydrate and ice adhesion calculation) [20,24,32]. Comparing to directly contacted bulb scale on glass, a sandwiched onion film leads to ~68% reduction in adhesion strength (from 312 kPa to 99 kPa). Therefore, the onion film can be an instructive bio-inspiring model for coating design for low adhesion strength.

With the effect of an onion film on adhesion strength discussed above, the corresponding mechanisms that can be utilized for mitigating hydrate adhesion are further explored. There are two key structural components in the onion film responsible for low adhesion, namely the surface cuticle layer and the sub-surface porous structure as depicted in Fig. 2a. The effects of onion film in lowering hydrate adhesion strength ($\tau_{hydrate}$) can be predicted using the empirical equation that widely used in design icephobic surfaces [23,33,42]

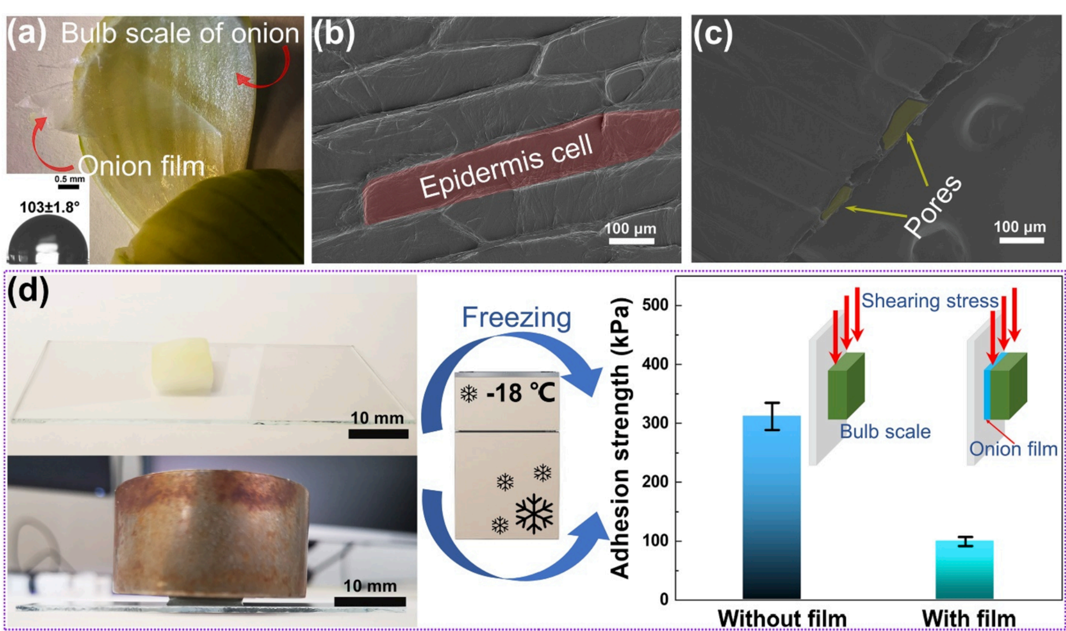

Fig. 1. Properties of onion films in lowering adhesion strength. (a) An onion film on a bulb scale of onion. The onion film is an intermediate epidermis between two bulb scales. The water contact angle on the film is shown as inset. (b) The corrugated surface morphology of an onion film. (c) The porous structures of an onion film shown by SEM image. The pores in the monolayer of epidermal cells are highlighted. (d) Samples of onion bulb scales with and without an onion film are cut into small pieces for quantifying their adhesion strength onto glass under −18 ℃ is measured.

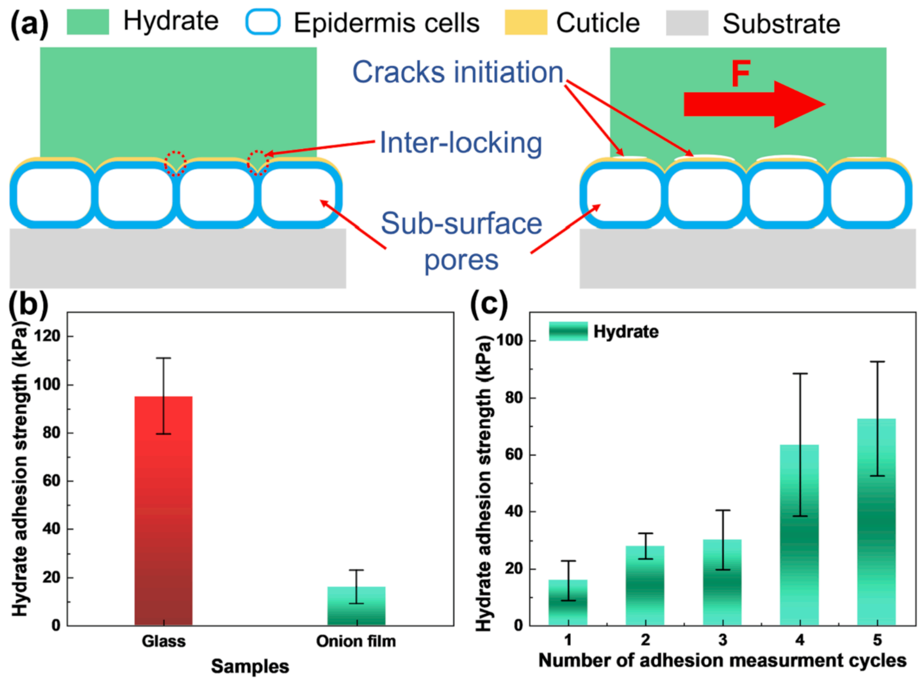

Fig. 2. Hydrate adhesion on onion films. (a) Schematic illustrations of hydrate-onion film system with and without external shearing force. (b) The hydrate adhesion strength on pure glass and glass that covered by onion film. (c) The hydrate adhesion strength on glass covered by onion film in hydrating/de-hydrating cycles. The hydrate adhesion strength is measured under −18 ℃ with CyC5 hydrate.

$$\tau_{hydrate} = \sqrt{\frac{E^{*}G}{\pi a \Lambda}}$$

where E^* is the apparent Young's modulus of surface, G is the surface energy, a is the total length of crack, and Λ is a nondimensional constant. Despite that the rough epidermal surface can potentially interlock with hydrate, the top cuticle layer of the onion film decreases surface energy G and at the same time can act as a lubricant for lowering hydrate adhesion [25]. On the other hand, the parameter a is affected by the micro-structures of an onion film. The unique sub-surface pores of the onion film can lead to stiffness inhomogeneity and initiate cracks at the hydrate-surface interface for facilitating hydrate removal [23,33,42,43]. Detail understanding on the crack initiation mechanisms through integrating sub-surface structures can be found in our previous works [23,42]. Importantly, the onion film maintains its flexibility even at low temperature of −18 ℃ (Supplementary Fig. S3), which is highly beneficial for crack initiation at the hydrate adhesion interface. Both the reduction in surface energy G and the initiation of interfacial cracks (i.e. increase in the value of a) contribute to the lower $\tau_{hydrate}$ on the onion film. It should be noted that the interstitial fluid in the epidermal cells of the onion film becomes ice under subzero temperature, which increase the surface modulus and could lead to strong hydrate-surface interactions. However, the possible counter effect of increased surface modulus is suppressed by the unique properties of surface chemistry and sub-surface structures. Overall, low hydrate adhesion strength on onion films is achieved. As shown in Fig. 2b, the CyC5 hydrate adhesion strength drastically decreases from 95 kPa on bare glass to 16 kPa on onion film coatings.

Although the mechanism of low hydrate adhesion is highly encouraging, the onion film has intrinsic weakness in hydrate mitigation applications. The surface cuticle can be depleted in an only handful cycles of adhesion test, which leads to the total failure of the onion film. Particularly, the CyC5 is a very destructive organic solvent which will intensify the consuming of surface cuticle. In some cases, wrinkles or even holes are observed on the tested surfaces. Strong mechanical interlocking exists between the hydrate and rough/broken epidermal surface. Subsequently, the hydrate adhesion strength on the broken onion film increases to 73 kPa after 5 cycles of hydrate adhesion test, which approaches to the hydrate adhesion on a glass. Similar increasing trends in ice adhesion strength are also observed on onion film samples in icing/de-icing cycles (Supplementary Fig. S4). Thanks to the relatively low destructive nature of water comparing to that of CyC5 solution, the ice adhesion on an onion film still remains far below that on a glass after 5 cycles. Nevertheless, the degradation of a real onion film is almost unavoidable due to the weak mechanical/chemical resistance in practice. Therefore, it is wise to realize the low hydrate adhesion mechanism of onion film in more durable materials for practical applications, namely fabricating novel onion inspired anti-hydrate surfaces.

2.2. Onion inspired surface with excellent hydrate-phobicity

Featuring the two key components of the onion film, the sub-surface pores and the top cuticle layer, is crucial for low hydrate adhesion. Using robust polymer-based materials, the novel onion inspired anti-hydrate coating is fabricated in a step-by-step approach, namely realizing the sub-surface pore structure first followed by enabling the function of the cuticle layer in the real onion films.

There are numbers of methods for fabricating a variety of porous materials, all of which can be used for creating similar sub-surface pores of the onion film [23,24]. For the sake of simplicity, a commercially available and robust polymer-based material, the gecko tape, is taken as an initial component for assembling a novel anti-hydrate coating. The gecko tape, originally designed for realizing special adhesion, has uniform pillars with interval distance of around 100 μm that is similar to the pore dimension in the onion film. As shown in Fig. 3a–c, applying the gecko tape on solid surfaces is a straight-forward but effective way of creating sub-surface pores like onion films. The face with pillars can firmly adhere on the substrate and create sub-surface pores, meanwhile, the smooth face can eliminate mechanical interlocking between hydrate and surface, as shown in Fig. 3d. It is worth emphasizing that other sub-surface pore structure by other fabrication method will serve the same purpose of fabricating the onion-inspired coating. Nevertheless, the choice of gecko tape in this work is sufficient to demonstrate the bio-inspired mechanisms for anti-hydrate. Furthermore, the as-prepared

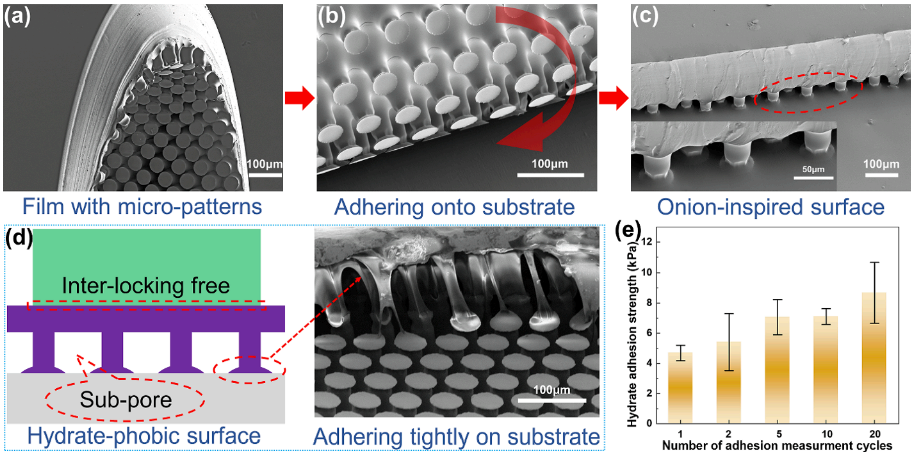

Fig. 3. Onion inspired anti-hydrate surfaces. (a) The microscope pillar structures of the gecko tape used as template for create sub-surface pore structures to mimic onion films. (b) The as-prepared film with uniform micro-pillars adhering onto a glass substrate. The interval distance of the pillars is close to the dimension of the pores in onion films. (c) The resulted onion inspired anti-hydrate coating has a smooth top surface and well-organized sub-surface pores. (d) Schematics of the onion inspired hydrate-phobic surface with the advantage of strong adhesion to various solid substrates. (e) The hydrate adhesion strength on the onion inspired coating in cyclic de-hydrate test. The hydrate adhesion strength is measured under −18 °C with CyC5 hydrate.

onion inspired coating has the advantage of enhanced adhesion to various solid substrates (different pipe walls), thanks to the micropillars mimicking the adhesion effect of gecko toe [44,45]. In a peeling off test, the micropillars are found to indeed adhere tightly on glass substrate (Fig. 3d). The strong adhesion between onion inspired film and substrate guarantees a stable coating, which is crucial for practical applications. The hydrate-phobicity of this new coating with sub-surface pores like those in onion films is then subjected to hydrate adhesion test. The hydrate adhesion strength on this onion inspired surface is extremely low, showing a mean value of around 4.7 kPa (Fig. 3e) and being more than 95 % reduction than the hydrate adhesion strength on a pure glass (Fig. 2b). As cyclic test results shown in Fig. 3e, the hydrate adhesion strength on the new coating maintains at a super low range, yielding an average value around 8.7 kPa after 20 hydrating/de-hydrating cycles. The new onion inspired coating also exhibits long-term low ice adhesion strength, as shown by results given in Supplementary Fig. S5. All the results here indicate that the onion inspired surface with sub-surface pore structure, one of the two key factors of onion film, can already greatly reduce hydrate adhesion strength and at the same time possess excellent durability.

The second property of an onion film that is crucial to hydrate removal is the cuticle layer on the surface. As discussed above, the cuticle layer can lower the surface energy and at the same time serve as surface lubricant, which provides further weakening effects on hydrate adhesion on top of the onion film. Here in this work, a regenerable low-energy lubricant layer is introduced on the as-prepared onion inspired coating to mimic the cuticle layer. As shown in Fig. 4a, the lubricating silicone oil is chosen for such purpose to infuse into the sub-surface porous structure of the onion inspired coating. The silicone oil can fill the sub-surface pores efficiently through self-diffusion that is driven by capillary forces [46]. Interestingly, the originally foggy onion inspired coating becomes highly transparent after lubricant infusing, as the details of the infusing process of the dyed lubricant depicted in Fig. 4a. With the silicone oil in the sub-surface pores as shown in Fig. 4b, the onion inspired coating (which is made of silicone elastomer) can gradually absorb the oil and constantly generate a thin lubricant layer atop unless the concentration gradient of the silicone oil is exhausted [47,48]. By integrating such regenerability of a top lubricant layer to mimicking cuticle layer on the onion film, the durability of anti-hydrate performance on the new coating is greatly enhanced, which is a sufficient way to avoid the failure of the real onion film as a result of consumption of the cuticle layer. It should be noted that the self-driven infusing of the silicone oil into the sub-surface pores of the onion inspired coating also provides an effective way for the replenishing of the lubricants. Importantly, the strategy introduced here for creating the lubricant layer to mimic the function of the cuticle layer on the onion film do not counteract with the crack initiating at the surfaces but rather enhance weakening effect of hydrate adhesion (Fig. 4b). Thanks to the synergy between two effects of sub-surface pores and the lubricating layer on this onion inspired surfaces, extremely low hydrate adhesion strength is

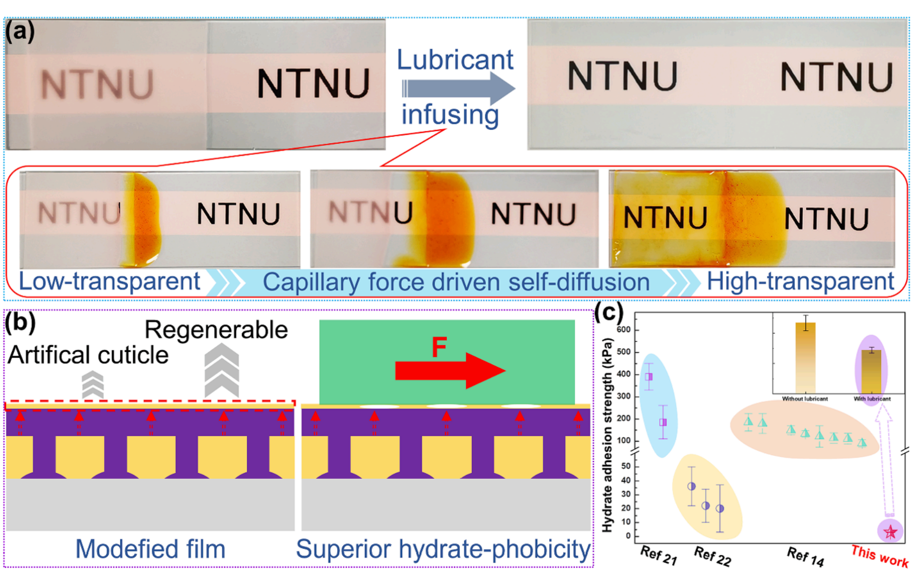

Fig. 4. Cuticle mimicking layer on the onion inspired coating with superior hydrate-phobicity. (a) High transparency of the coating with infused lubricant in the sub-surface pores. The detailed self-diffusion process of lubricant infusing driven by capillary force is shown by dyed silicone oil. (b) Schematics of the regenerability of the lubricant layer and the resulting superior hydrate-phobicity. (c) The comparison chart that shows the hydrate adhesion strength in the literatures and in this work. The hydrate adhesion strength on the onion inspired surfaces with and without artificial cuticles are inserted. The hydrate adhesion strength is measured under −18 °C with CyC5 hydrate.

realized on the coating, reaching an unprecedented low hydrate adhesion strength of 2.9 kPa as shown in Fig. 4c. Given that the lubricant layer can be generated continuously with an adequate source of supply, the hydrate adhesion on the onion inspired coatings will be maintained at extremely low values. However, in the practical oil/gas transportations, the liquid lubricant can be depleted fast under the fluid washing. Moreover, the replenishment of the lubricant in a real pipeline system can be challenging. Future design that can provide long-term surface lubricating effects without replenishing is highly needed. With a comparison chart shown in Fig. 4c, we know that our onion inspired strategy provides the lowest hydrate adhesion strength comparing to other reports [14,21,22]. However, one should note that different test conditions (including apparatus' set-up, temperatures, hydrate types, and so on) are applied in various studies. Further studies on the hydrate adhesion strength using a standardized test condition, especially, with methane hydrate will be essential for promoting hydrate-phobic surfaces to practical applications. We also would like to point out that in the oil/gas transportation systems, the adhesion behaviors between hydrate and surfaces can be more complicated by taking the water layer above the hydrate particles into consideration [49]. Aspects concerning muti-scale hydrate adhesion strength calculation, water layer effects on the hydrate adhesion, subcooling effects on hydrate adhesion, and hydrate adhesion of various hydrates need to be systematically investigated in the near future.

2.3. Conclusions

In this work, the mechanisms of the exceptional performance of onion film in lowering adhesion strength is explored, and further applied in fabricating an onion inspired surface with superior low hydrate adhesion strength. Specifically, the sub-surface pores and the atop cuticle layer are found accountable for the low hydrate adhesion. The sub-surface porous structures can cause stiffness inhomogeneity and initiate interface cracks, while the cuticle can act as hydrophobic lubricating layer for further lowering hydrate adhesion. An onion inspired surface is then fabricated to mimicking the low hydrate adhesion functionality of the onion film, with special care taken to enhance the materials durability. By creating a smooth surface with sub-surface pores on robust elastomer, the new onion inspired coating achieves extremely low hydrate adhesion strength of 2.9 kPa. The onion inspired surface can also maintain excellent hydrate-phobicity with low hydrate adhesion strength of 8.7 kPa after 20 hydrating/de-hydrating cycles. The surface designed with this regenerable slippery lubricating layer shows outstanding hydrate-phobicity, thus possesses great potentials for practical anti-hydrate applications. The in-depth bio-inspiring strategy in this work also opens an avenue for the fabrication of new anti-hydrate materials.

3. Materials and methods

3.1. Materials

Fresh onions that are bought from supermarket are used for the tests. The actual onion films and onion bulb scales are peeled off and used for the adhesion and water contact angle test. The onion inspired surfaces are fabricated by paste elastomer films (Gecko® Nanoplast®, Germany) onto glass substrates. To create the lubricant layer on the onion inspired coating, silicone oil (Sigma Aldrich, Germany) is infused into the sub-surface pores. The silicone oil colored with Sudan I (Sigma Aldrich, Germany) is used to show the diffusion process of oil into the sub-surface pores. The precursor of CyC5 hydrate is fabricated by mixing cyclopentane with deionized water using the method reported by McKinley et al. [22]. Firstly, 4 wt% Tween 85 (Sigma-Aldrich, Germany) is dissolved in water to serve as an emulsifier. The cyclopentane is then added into water, the CyC5-to-water molar ratio is fixed at 1: 17. The mixture is further handled with 30 min of ultrasonication to obtain the CyC5-in-water emulsion.

3.2. Fabrication of coatings

The onion films are peeled off from the bulb scales and are adhered onto glass substrates for ice/hydrate adhesion tests. In adhering an onion film onto a glass, the hydrophilic side (Supplementary Fig. S2) is brought into contact with the substrate and the hydrophobic side of the onion film is exposed for ice/hydrate adhesion test. To ensure a tight contact between an onion film and a glass surface, a transparent double-side tap is used as an intermediate layer. The onion films are carefully adhered with a smooth contact to the glass substrate. The onion inspired surface is made by coating elastomer films with smooth surface and sub-surface micro-pillars onto glass substrates. The elastomer film is a commercially available gecko tap that provided by the Gottlieb Binder GmbH & Co. KG. The fabrication method of this tap is not included in this work. The well-designed gecko feet inspired pillars can adhered perfectly and tightly onto glass substrates. After infusing the silicone oil into the sub-surface pores, the lubricant can gradually penetrate the elastomer and form an artificial cuticle layer on the coatings. The surfaces after silicone oil infusing are stored in room temperature for 24 h before hydrate adhesion measurements.

3.3. Characterizations

The morphologies of the onion films and onion inspired surfaces are characterized by a field-emission scanning electron microscope (FEI APREO SEM). The onion film is pre-dried in fume hood for 10 days under room temperature before SEM observation. All samples are sputter-coated with a 10 nm platinum/palladium layer before SEM characterization. The water contact angle is measured using a CAM 200 contact-angle system (KSV Instruments Ltd., Helsinki, Finland), where water is supplied via a syringe in or out of sessile droplets (~2 μL). The fresh surfaces of onion film and onion bulb scale are held under room temperature for 1 h to evaporate the surface water before water contact angle test. To measure the adhesion strength between onion bulb scales and glass substrates, the bulb scales are firstly cut into samples with a dimension of 10 mm * 10 mm * 2 mm. Then, the bulb scales are pasted onto the glass substrates. A weight around ~200 g is placed atop the bulb scales to ensure a full contact between the samples and the glasses (Fig. 1d). Two adhesive systems are made, one with an intermediate onion film between bulb scale and glass substrate, and another one without an intermediate layer. The systems are then transferred into a freezer with a temperature of −18 °C for 3 h. The adhesion strength of frozen bulb scales on glass are measured by a universal mechanical tester (Instron Model 5944) equipped with lab built cooling system and chamber, as described in previous studies [23]. In order to test the adhesion strength of frozen bulb scales to glasses, the prob is placed on the bulb scales directly. The ice/hydrate adhesion strength is also measured using the same instrument and set-up. A polypropylene centrifuge tube with a 1 mm thick wall and a 15 mm inner diameter is placed on the coatings. 1.5 mL deionized water is infused into the mold, the samples are then held in freezer with constant temperature of −18 °C for 3 h to ensure complete freezing. To prepare a hydrate sample, 1.5 mL CyC5-in-water emulsion is infused into the mold and held under −18 °C for 6 h (Supplementary Fig. S6). Before test, the samples are transferred from the freezer to the cooling chamber of the test machine and stabilized at −18 °C for 30 min. During adhesion test, a force probe propels the adhered samples at a velocity of 0.01 mm·s − 1, and the probe is located close to the tested coating surface (<1 mm) to minimize the torque on the ice/hydrate cylinder. 5 samples for each type of adhesion test are prepared to get an average adhesion strength.

Declaration of Competing Interest

The authors declare that they have no known competing financial

interests or personal relationships that could have appeared to influence the work reported in this paper.

Acknowledgements

The Research Council of Norway is acknowledged for the support to the NANO2021 project Dual-Functional Anti-Gas Hydrate Surfaces (DAndra, 302348), the support to the FRIPRO project Towards Design of Super-Low Ice Adhesion Surfaces (SLICE, 250990), and the support to the Norwegian Micro- and Nano-Fabrication Facility, NorFab (295864).

Appendix A. Supplementary data

Supplementary data to this article can be found online at https://doi.org/10.1016/j.cej.2022.135274.

References

[1] E.D. Sloan Jr., C.A. Koh, C.A. Koh (Eds.), Clathrate Hydrates of Natural Gases, CRC Press, 2007.
[2] A. Hassanpouryouzband, E. Joonaki, M. Vasheghani Farahani, S. Takeya, C. Ruppel, J. Yang, N.J. English, J.M. Schicks, K. Edlmann, H. Mehrabian, Z. M. Aman, B. Tohidi, Gas hydrates in sustainable chemistry, Chem. Soc. Rev. 49 (15) (2020) 5225–5309.
[3] H. Ganji, M. Manteghian, K. Sadaghiani zadeh, M.R. Omidkhah, H. Rahimi Mofrad, Effect of different surfactants on methane hydrate formation rate, stability and storage capacity, Fuel 86 (3) (2007) 434–441.
[4] P. Babu, P. Linga, R. Kumar, P. Englezos, A review of the hydrate based gas separation (HBGS) process for carbon dioxide pre-combustion capture, Energy 85 (2015) 261–279.
[5] J.-N. Zheng, M. Yang, Experimental investigation on novel desalination system via gas hydrate, Desalination 478 (2020), 114284.
[6] E.D. Sloan, Natural gas hydrates in flow assurance, Gulf Professional Publishing (2010).
[7] Z. Wang, Y. Zhao, J. Zhang, S. Pan, J. Yu, B. Sun, Flow assurance during deepwater gas well testing: Hydrate blockage prediction and prevention, J. Petrol. Sci. Eng. 163 (2018) 211–216.
[8] A.K. Sum, C.A. Koh, E.D. Sloan, Clathrate hydrates: from laboratory science to engineering practice, Industrial & Engineering Chemistry Research 48 (16) (2009) 7457–7465.
[9] A.K.M. Jamaluddin, N. Kalogerakis, P.R. Bishnoi, Hydrate plugging problems in undersea natural gas pipelines under shutdown conditions, J. Petrol. Sci. Eng. 5 (4) (1991) 323–335.
[10] A. Bozorgian, A. Samimi, A review of Kinetics of Hydrate Formation and the Mechanism of the Effect of the inhibitors on it, International Journal of New, Chemistry (2020).
[11] T. Yagasaki, M. Matsumoto, H. Tanaka, Effects of thermodynamic inhibitors on the dissociation of methane hydrate: a molecular dynamics study, PCCP 17 (48) (2015) 32347–32357.
[12] M.A. Kelland, History of the development of low dosage hydrate inhibitors, Energy Fuels 20 (3) (2006) 825–847.
[13] C.N. Khalil, N.D.O. Rocha, L.C.F. Leite, Process for the thermo-hydraulic control of gas hydrates, Google Patents (2000).
[14] J.D. Smith, A.J. Meuler, H.L. Bralower, R. Venkatesan, S. Subramanian, R. E. Cohen, G.H. McKinley, K.K. Varanasi, Hydrate-phobic surfaces: fundamental studies in clathrate hydrate adhesion reduction, PCCP 14 (17) (2012) 6013–6020.
[15] E.D. Sloan, Fundamental principles and applications of natural gas hydrates, Nature 426 (6964) (2003) 353–359.
[16] S. Fan, H. Zhang, G. Yang, Y. Wang, G. Li, X. Lang, Reduction Clathrate Hydrates Growth Rates and Adhesion Forces on Surfaces of Inorganic or Polymer Coatings, Energy Fuels 34 (11) (2020) 13566–13579.
[17] H. Sojoudi, H. Arabnejad, A. Raiyan, S.A. Shirazi, G.H. McKinley, K.K. Gleason, Scalable and durable polymeric icephobic and hydrate-phobic coatings, Soft Matter 14 (18) (2018) 3443–3454.
[18] W. Zhang, S. Fan, Y. Wang, X. Lang, G. Li, Preparation and performance of biomimetic superhydrophobic coating on X80 pipeline steel for inhibition of hydrate adhesion, Chem. Eng. J. 419 (2021), 129651.
[19] T. Ragunathan, X. Xu, J.A. Shuhili, C.D. Wood, Preventing Hydrate Adhesion with Magnetic Slippery Surfaces, ACS Omega 4 (14) (2019) 15789–15797.
[20] R. Ma, F. Wang, Y. Chang, S. Xiao, N.J. English, J. He, Z. Zhang, Unraveling Adhesion Strength between Gas Hydrate and Solid Surfaces, Langmuir 37 (47) (2021) 13873–13881.
[21] H. Sojoudi, M.R. Walsh, K.K. Gleason, G.H. McKinley, Designing Durable Vapor-Deposited Surfaces for Reduced Hydrate Adhesion, Adv. Mater. Interfaces 2 (6) (2015) 1500003, https://doi.org/10.1002/admi.201500003.
[22] H. Sojoudi, M.R. Walsh, K.K. Gleason, G.H. McKinley, Investigation into the formation and adhesion of cyclopentane hydrates on mechanically robust vapor-deposited polymeric coatings, Langmuir 31 (22) (2015) 6186–6196.
[23] Z. He, S. Xiao, H. Gao, J. He, Z. Zhang, Multiscale crack initiator promoted super-low ice adhesion surfaces, Soft Matter 13 (37) (2017) 6562–6568.
[24] F. Wang, S. Xiao, Y. Zhuo, W. Ding, J. He, Z. Zhang, Liquid layer generators for excellent icephobicity at extremely low temperatures, Mater. Horiz. 6 (10) (2019) 2063–2072.
[25] A. Das, T.A. Farnham, S. Bengaluru Subramanyam, K.K. Varanasi, Designing ultra-low hydrate adhesion surfaces by interfacial spreading of water-immiscible barrier films, ACS Appl. Mater. Interfaces 9 (25) (2017) 21496–21502.
[26] E. Brown, S. Hu, S. Wang, J. Wells, M. Nakatsuka, V. Veedu, C. Koh, Low-adhesion coatings as a novel gas hydrate mitigation strategy, Offshore Technology Conference, OnePetro (2017).
[27] S. Dong, M. Li, C. Liu, J. Zhang, G. Chen, Bio-inspired Superhydrophobic Coating with Low Hydrate Adhesion for Hydrate Mitigation, Journal of Bionic Engineering 17 (5) (2020) 1019–1028.
[28] M.A. Pickarts, J. Delgado-Linares, E. Brown, V. Veedu, C.A. Koh, Surface Treatment Strategies for Mitigating Gas Hydrate & Asphaltene Formation, Growth, and Deposition in Flowloops, Offshore Technology Conference, OnePetro (2021).
[29] S. Farhadi, M. Farzaneh, S.A. Kulinich, Anti-icing performance of superhydrophobic surfaces, Appl. Surf. Sci. 257 (14) (2011) 6264–6269.
[30] Y. Wang, J. Xue, Q. Wang, Q. Chen, J. Ding, Verification of icephobic/anti-icing properties of a superhydrophobic surface, ACS Appl. Mater. Interfaces 5 (8) (2013) 3370–3381.
[31] J. Chen, J. Liu, M. He, K. Li, D. Cui, Q. Zhang, X. Zeng, Y. Zhang, J. Wang, Y. Song, Superhydrophobic surfaces cannot reduce ice adhesion, Appl. Phys. Lett. 101 (11) (2012) 111603, https://doi.org/10.1063/1.4752436.
[32] F. Wang, R. Ma, S. Xiao, N.J. English, J. He, Z. Zhang, Anti-gas hydrate surfaces: perspectives, progress and prospects, J. Mater. Chem. A (2022).
[33] F. Wang, Y. Zhuo, Z. He, S. Xiao, J. He, Z. Zhang, Dynamic Anti-Icing Surfaces (DAIS), Advanced, Science 8 (21) (2021) 2101163, https://doi.org/10.1002/advs.v8.2110.1002/advs.202101163.
[34] J. Lv, Y. Song, L. Jiang, J. Wang, Bio-inspired strategies for anti-icing, ACS Nano 8 (4) (2014) 3152–3169.
[35] L. Mishchenko, B. Hatton, V. Bahadur, J.A. Taylor, T. Krupenkin, J. Aizenberg, Design of ice-free nanostructured surfaces based on repulsion of impacting water droplets, ACS Nano 4 (12) (2010) 7699–7707.
[36] P. Kim, T.-S. Wong, J. Alvarenga, M.J. Kreder, W.E. Adorno-Martinez, J. Aizenberg, Liquid-infused nanostructured surfaces with extreme anti-ice and anti-frost performance, ACS Nano 6 (8) (2012) 6569–6577.
[37] C.-C. Chen, W.-P. Shih, P.-Z. Chang, H.-M. Lai, S.-Y. Chang, P.-C. Huang, H.-A. Jeng, Onion artificial muscles, Appl. Phys. Lett. 106 (18) (2015) 183702, https://doi.org/10.1063/1.491749810.1063/1.4917498.1.
[38] A. Ng, M.L. Parker, A.J. Parr, P.K. Saunders, A.C. Smith, K.W. Waldron, Physicochemical characteristics of onion (Allium cepa L.) tissues, J. Agric. Food. Chem. 48 (11) (2000) 5612–5617.
[39] M.S. Zamil, H. Yi, V.M. Puri, A multiscale FEA framework for bridging cell-wall to tissue-scale mechanical properties: the contributions of middle lamella interface and cell shape, J. Mater. Sci. 52 (13) (2017) 7947–7968.
[40] T. Tantamacharik, S.Y. Leong, M.J. Leus, G.T. Eyres, D.J. Burritt, I. Oey, Structural changes induced by pulsed electric fields increase the concentration of volatiles released in Red Onion (Allium cepa L. var, Red Pearl) Bulbs, Foods 8 (9) (2019) 368.
[41] R. Jetter, L. Kunst, A.L. Samuels, Composition of plant cuticular waxes, Biol. Plant Cuticle 23 (2008) 145–181.
[42] Z. He, Y. Zhuo, F. Wang, J. He, Z. Zhang, Design and preparation of icephobic PDMS-based coatings by introducing an aqueous lubricating layer and macro-crack initiators at the ice-substrate interface, Prog. Org. Coat. 147 (2020), 105737.
[43] F. Wang, W. Ding, J. He, Z. Zhang, Phase transition enabled durable anti-icing surfaces and its DIY design, Chem. Eng. J. 360 (2019) 243–249.
[44] J. Davies, S. Haq, T. Hawke, J.P. Sargent, A practical approach to the development of a synthetic Gecko tape, Int. J. Adhes. Adhes. 29 (4) (2009) 380–390.
[45] M. Zhou, N. Pesika, H. Zeng, Y.u. Tian, J. Israelachvili, Recent advances in gecko adhesion and friction mechanisms and development of gecko-inspired dry adhesive surfaces, Friction 1 (2) (2013) 114–129.
[46] W. Pei, J. Li, Z. Guo, Y. Liu, C. Gao, L. Zhong, S. Wang, Y. Hou, Y. Zheng, Excellent fog harvesting performance of liquid-infused nano-textured 3D frame, Chem. Eng. J. 409 (2021), 128180.
[47] Y. Wang, X.i. Yao, S. Wu, Q. Li, J. Lv, J. Wang, L. Jiang, Bioinspired solid organogel materials with a regenerable sacrificial alkane surface layer, Advanced Materials 29 (26) (2017) 1700865, https://doi.org/10.1002/adma.v29.2610.1002/adma.201700865.
[48] Y. Zhuo, F. Wang, S. Xiao, J. He, Z. Zhang, One-step fabrication of bioinspired lubricant-regenerable icephobic slippery liquid-infused porous surfaces, ACS Omega 3 (8) (2018) 10139–10144.
[49] H. Liang, D. Guan, K. Shi, L. Yang, L. Zhang, J. Zhao, Y. Song, Characterizing mass-transfer mechanism during gas hydrate formation from water droplets, Chem. Eng. J. 428 (2022), 132626.